

New investigations within the TeO_2 -rich part of the $\text{Tl}_2\text{O}-\text{TeO}_2$ system

Barbara Jeansannetas, Pascal Marchet, Philippe Thomas, Jean Claude Champarnaud-Mesjard and Bernard Frit

Laboratoire de Matériaux Céramiques et Traitements de Surface, ESA-CNRS 6015, Université de Limoges, Faculté des Sciences, 123 avenue Albert-Thomas, 87060 Limoges Cedex, France

The phase diagram TeO_2 - Tl_2TeO_3 has been studied under equilibrium and non-equilibrium conditions by differential scanning calorimetry and temperature programmed X-ray diffraction. Four crystalline phases, three stable (Tl_2TeO_3 , α - $\text{Tl}_2\text{Te}_2\text{O}_5$, $\text{Tl}_2\text{Te}_3\text{O}_7$) and one metastable (β - $\text{Tl}_2\text{Te}_2\text{O}_5$) have been identified and characterized. The three stable phases decompose peritectically at 377, 315 and 342 °C respectively. β - $\text{Tl}_2\text{Te}_2\text{O}_5$, which is formed by cooling of a melt, undergoes a monotropic transformation into the stable α polymorph. This study also confirmed the existence of a large glass-forming domain (15–52 mol% $\text{TlO}_{0.5}$). The complex thermal behaviour of these very stable glasses has been studied. The glass transition and crystallization temperatures, and the nature of crystalline phases formed, have been determined.

The increasing interest for materials with non-linear optical properties has been induced by the important industrial request for 'all-optical' devices. Glasses are very good potential candidates for such applications because of their malleability, their homogeneity in a wide range of compositions and their chemical stability. Tellurium dioxide-based glasses are of special interest due to their high linear and non-linear refractive indices and their good visible and infrared light transmittance.^{1,2} The stereochemical activity of the Te^{IV} atoms is certainly at the origin of such properties. It is very often reinforced when a second lone pair holder is associated with the Te^{IV} atoms. From this point of view investigations within the $\text{Tl}_2\text{O}-\text{TeO}_2$ system were of prime importance. Previous studies concerning this system have revealed the existence of: (i) four stoichiometric crystalline compounds: Tl_2TeO_3 , α - and β - $\text{Tl}_2\text{Te}_2\text{O}_5$, and $\text{Tl}_2\text{Te}_3\text{O}_7$;³ (ii) a large glassy domain whose proposed composition range greatly differed from one author to the other,^{1,4-7} probably because of different experimental conditions.

An equilibrium phase diagram has been proposed for compositions ranging from TeO_2 to Tl_2TeO_3 .⁸ However, this is obviously wrong, since none of the four ternary compounds, Tl_2TeO_3 , α - and β - $\text{Tl}_2\text{Te}_2\text{O}_5$, and $\text{Tl}_2\text{Te}_3\text{O}_7$, is indicated.

The aim of this study was to accurately determine on the one hand the phase diagram in equilibrium and non-equilibrium conditions for the pseudo-binary Tl_2TeO_3 - TeO_2 system, and on the other hand the thermal behaviour of the glasses.

Experimental

All the crystallized samples were obtained by heating, at 350 °C for 18 h then at 250 °C for 24 h, in a gold crucible under pure flowing nitrogen, various mixtures of high purity Tl_2CO_3 and TeO_2 . Tl_2CO_3 was a commercial product (Aldrich, 99.9%) and TeO_2 was prepared by decomposition, at 550 °C under flowing oxygen, of commercial H_6TeO_6 (Aldrich).

Glassy samples were prepared by first melting at 800 °C in sealed gold tubes, and then air-quenching, intimate mixtures of Tl_2TeO_3 and TeO_2 . Glass formation domain and crystallized phase compositions were determined by using X-ray diffraction (Guinier-De Wolff camera, Cu-K α radiation). The structural evolution with temperature of the crystallized compounds and glasses was followed by *in situ* X-ray powder diffraction (XRPD) with a Siemens D5000 diffractometer (θ/θ mode, Cu-

K α radiation) fitted with a high temperature furnace (Anton-Parr HTK10), a platinum heating sample holder (a gold sheet was added on the platinum sample holder to avoid reactions between the sample and platinum) and an Elphyse position sensitive detector (14° aperture). The heating rate was 10 °C min⁻¹ and each XRPD pattern was recorded after an annealing time of 10 min at the chosen temperature, in the 2θ range 14–90° (step size: 0.029, time range: 15 min). Phase transformation, glass transition (T_g), crystallization (T_c) and melting (T_f) temperatures were measured by heat flux differential scanning calorimetry (DSC; DSC Netzsch STA 409). The powdered samples (*ca.* 30 mg) were introduced into covered gold crucibles and the DSC curves were recorded between 20 and 800 °C using a heating rate of 10 °C min⁻¹ and a pure nitrogen atmosphere. The glass transition temperature was taken as the inflection point of the step change of the calorimetric signal associated with this transition. The crystallization temperature was taken (when an exothermic peak was observed which, as we will see, was very rare) as the intersection of the slope of this exothermic peak with the baseline. As for the liquidus temperature, T_l , it was considered to correspond to the bottom of the related endothermic peak. The energies of the different thermal events were obtained from the area under the corresponding peak after heat-flow rate calibration (calibration substance: sapphire).

The densities of both crystalline and glassy samples were measured on finely ground powders by helium pycnometry (Accupyc 1330 pycnometer).

Results and Discussion

Equilibrium phase diagram

Our investigations confirmed the existence of the four crystalline compounds previously reported: three stable phases (Tl_2TeO_3 , α - $\text{Tl}_2\text{Te}_2\text{O}_5$ and $\text{Tl}_2\text{Te}_3\text{O}_7$) and one metastable phase (β - $\text{Tl}_2\text{Te}_2\text{O}_5$).

The corresponding phase equilibrium diagram is shown in Fig. 1. It comprises four invariant equilibria: one eutectic and three peritectic reactions. The eutectic reaction ($E = 55$ mol% $\text{TlO}_{0.5}$, $T_E = 309 \pm 5$ °C, $\Delta H_E = 106 \pm 2$ kJ mol⁻¹) corresponds to the equilibrium: $L_E \rightleftharpoons \text{Tl}_2\text{TeO}_3 + \alpha\text{-Tl}_2\text{Te}_2\text{O}_5$. The first peritectic reaction, P_1 , corresponds to the incongruent melting, at 377 ± 5 °C, of the Tl_2TeO_3 compound ($\Delta H_p = 15 \pm 2$ kJ mol⁻¹) and to the equilibrium: $\text{Tl}_2\text{TeO}_3 \rightleftharpoons L_{P_1} + \text{unidentified solid}$

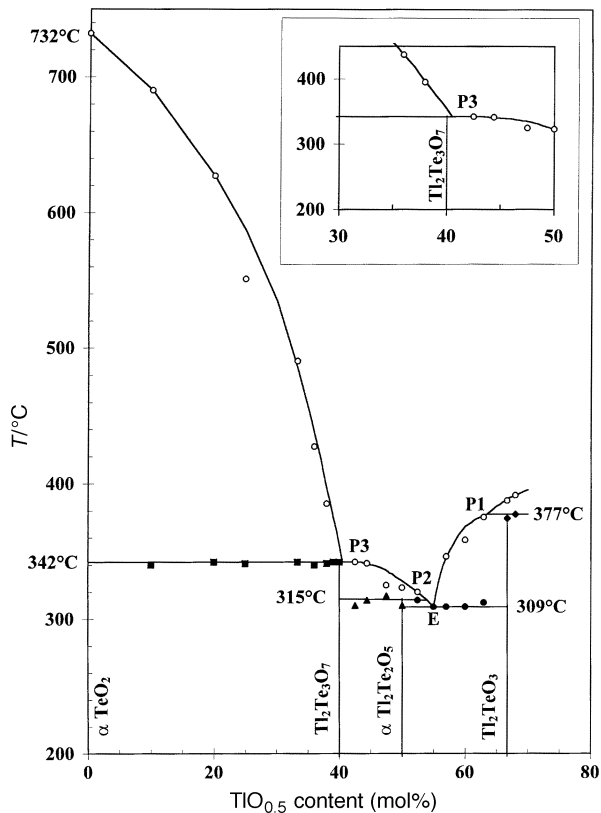


Fig.1 Equilibrium phase diagram of the TeO_2 - Tl_2TeO_3 system

phase. The second peritectic reaction, P_2 , corresponds to the incongruent melting at $315 \pm 5^\circ\text{C}$ of the stable form α of the $\text{Tl}_2\text{Te}_2\text{O}_5$ compound, according to the equilibrium: $\alpha\text{-Tl}_2\text{Te}_2\text{O}_5 \rightleftharpoons L_{P_2} + \text{Tl}_2\text{Te}_3\text{O}_7$. The third one, P_3 , corresponds to the quasi congruent melting, at $342 \pm 5^\circ\text{C}$, of the $\text{Tl}_2\text{Te}_3\text{O}_7$ compound ($\Delta H_p = 53 \pm 2 \text{ kJ mol}^{-1}$) and to the equilibrium:

$\text{Tl}_2\text{Te}_3\text{O}_7 \rightleftharpoons L_{P_3} + \alpha\text{-TeO}_2$. The enlarged-scale scheme shown as an insert in Fig. 1 visualizes the most probable equilibrium curves, even if thermal effects corresponding to peritectic and liquidus equilibria could not be experimentally separated.

Contrary to what was previously published,³ the $\beta\text{-Tl}_2\text{Te}_2\text{O}_5$ polymorph cannot be considered as the stable high-tempera-

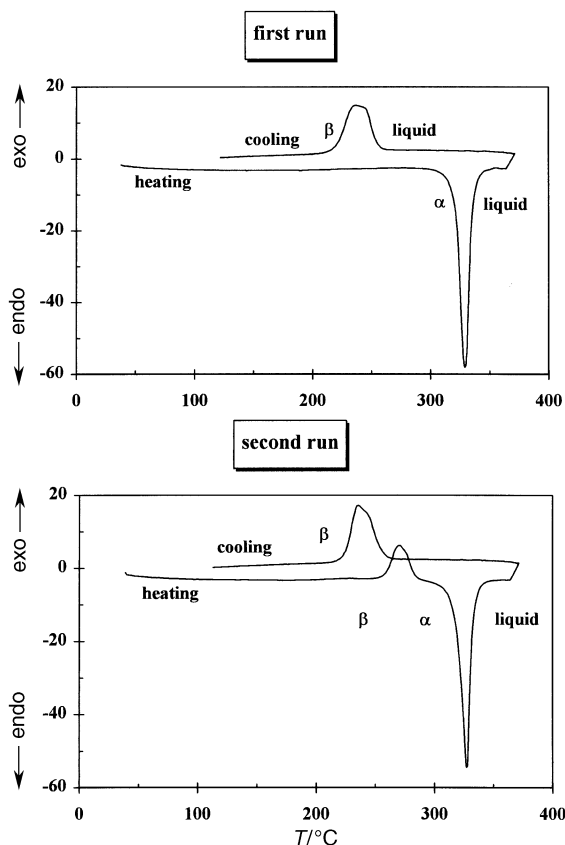


Fig. 2 DSC curves of crystalline $\alpha\text{-Tl}_2\text{Te}_2\text{O}_5$ (heating rate $10^\circ\text{C min}^{-1}$)

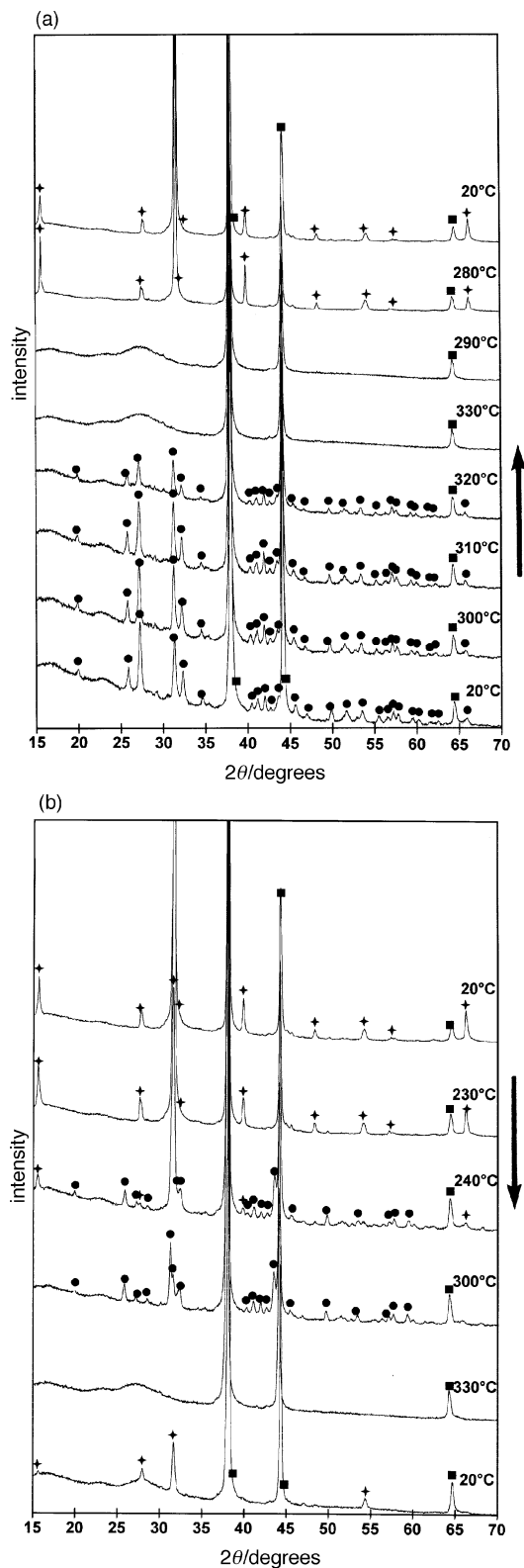


Fig. 3 XRD patterns at various temperatures of crystalline $\alpha\text{-Tl}_2\text{Te}_2\text{O}_5$ (a) first heating and cooling, (b) second heating and cooling (● $\alpha\text{-Tl}_2\text{Te}_2\text{O}_5$, + $\beta\text{-Tl}_2\text{Te}_2\text{O}_5$, ■ Au; heating and cooling rates of $10^\circ\text{C min}^{-1}$, annealing time of 10 min at each temperature, Au diffraction peaks are those of the gold sheet on the Pt sample holder)

ture form of $\text{Ti}_2\text{Te}_2\text{O}_5$ but, as is clearly shown by the DSC curves of Fig. 2 and the various XRPD patterns of Fig. 3 registered with an initial well crystallized $\alpha\text{-Ti}_2\text{Te}_2\text{O}_5$ sample, it is a metastable phase which is formed only during cooling of a liquid or glassy sample and which irreversibly and exothermically transforms, by heating at temperatures higher than 250°C , into the stable α -form.

Formation and thermal behaviour of glasses

Under our experimental conditions, the glass forming domain ranges from 15 to 52 mol% $\text{TiO}_{0.5}$. The glasses are all yellow, the intensity of the colour increasing with $\text{TiO}_{0.5}$ content. The density increases from about 5.9 to 7.1 with increasing $\text{TiO}_{0.5}$ content. These values are in perfect agreement with previously published ones.^{1,4-7}

The evolution with composition of the glass transition and crystallization temperatures is shown in Fig. 4. (Since, for

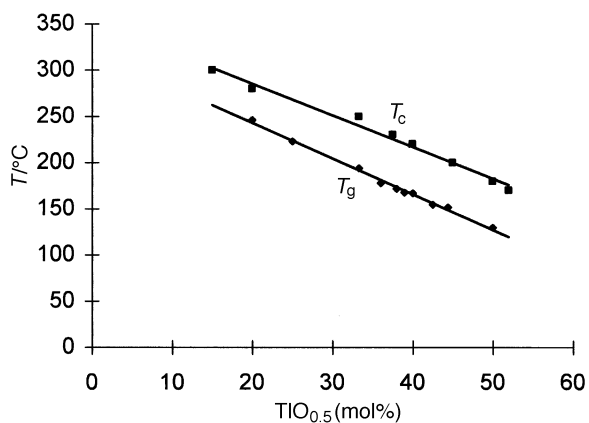


Fig. 4 Evolution with composition of the glass transition (T_g) and crystallization temperature (T_c) of the $\text{Ti}_2\text{O}-\text{TeO}_2$ glasses

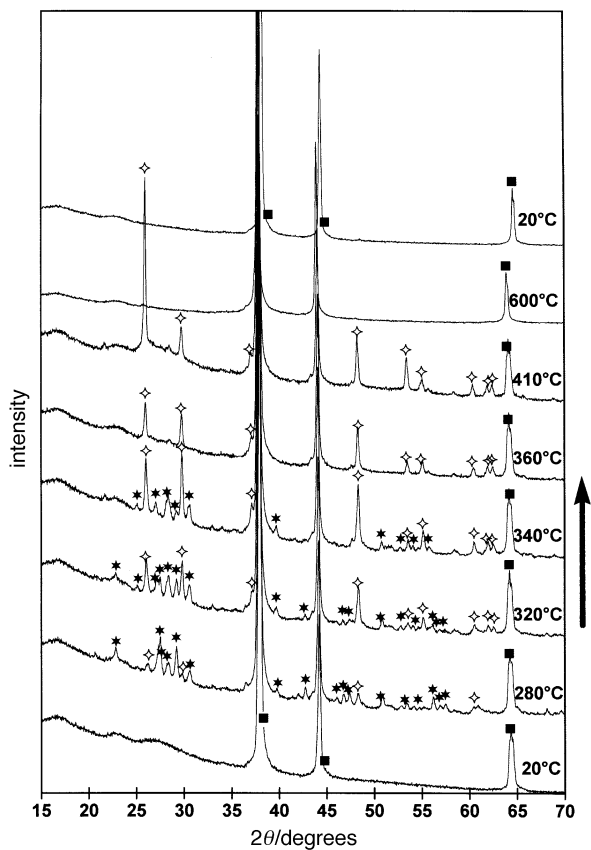


Fig. 5 XRD patterns at various temperatures of the 80 mol% TeO_2 -20 mol% $\text{TiO}_{0.5}$ glassy sample (* $\text{Ti}_2\text{Te}_3\text{O}_7$, \diamond $\alpha\text{-TeO}_2$, \blacksquare Au; Au diffraction peaks are those of the gold sheet on the Pt sample holder)

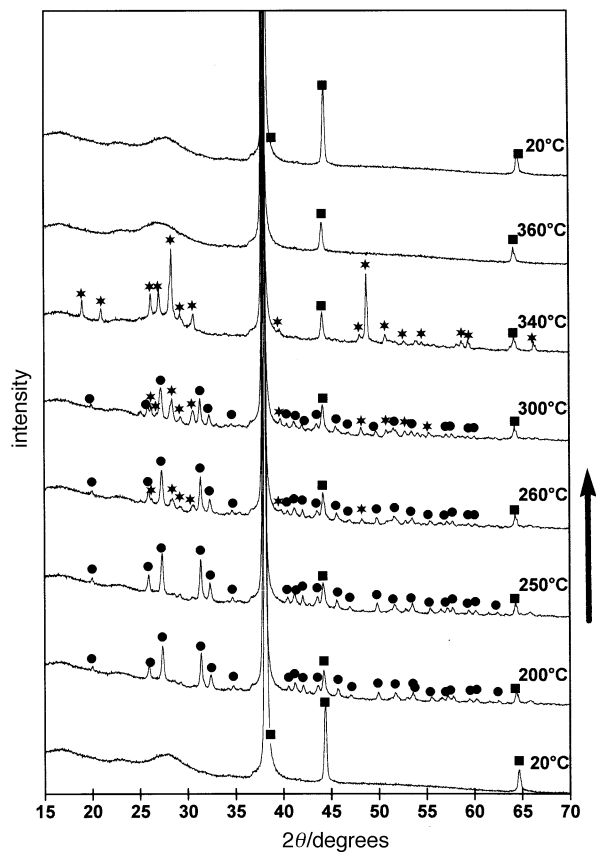


Fig. 6 XRD patterns at various temperatures of the 55 mol% TeO_2 -45 mol% $\text{TiO}_{0.5}$ glassy sample (\bullet $\alpha\text{-Ti}_2\text{Te}_2\text{O}_5$, * $\text{Ti}_2\text{Te}_3\text{O}_7$, \blacksquare Au; Au diffraction peaks are those of the gold sheet on the Pt sample holder)

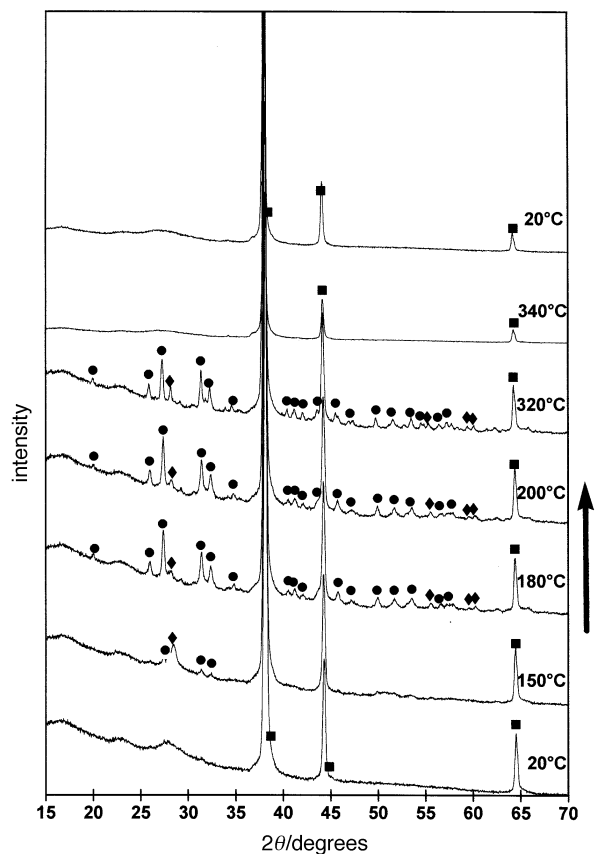


Fig. 7 XRD patterns at various temperatures of the 48 mol% TeO_2 -52 mol% $\text{TiO}_{0.5}$ glassy sample (\bullet $\alpha\text{-Ti}_2\text{Te}_2\text{O}_5$, \diamond Ti_2TeO_3 , \blacksquare Au; Au diffraction peaks are those of the gold sheet on the Pt sample holder)

nearly all the samples, no clearly defined exothermic peak was observed on the DSC curves, which confirms the high thermal stability of these glasses, the crystallization temperatures reported correspond to the temperatures from which the first XRD peaks were observed on temperature programmed XRPD patterns).

T_g and T_c decrease linearly with increasing $TiO_{0.5}$ content. For samples containing more than 15 and less than 40 mol% $TiO_{0.5}$ (see for example the XRPD patterns at various temperatures of the sample with 20 mol% $TiO_{0.5}$ shown in Fig. 5) α - TeO_2 and $Tl_2Te_3O_7$ crystals are formed simultaneously, the proportions of the latter increasing with increasing $TiO_{0.5}$ content. With increasing temperature both crystals disappear: above 340 °C for the $Tl_2Te_3O_7$ crystals, as soon as the liquidus temperature is reached for the α - TeO_2 crystals.

For samples in the range 40–50 mol% $TiO_{0.5}$ (Fig. 6), we first observe the crystallization of the stable α - $Tl_2Te_2O_5$ polymorph, at temperatures ranging from 220 to 180 °C and then the formation of $Tl_2Te_3O_7$ crystals at about 260 °C.

For the composition 50% TeO_2 –50% $TiO_{0.5}$ (composition corresponding to that of the $Tl_2Te_2O_5$ compound), α - $Tl_2Te_2O_5$ crystals are formed from 180 °C. They disappear by melting above 315 °C. Small quantities of β - $Tl_2Te_2O_5$ are formed during the rapid cooling of the melt, confirming that this metastable phase can only be formed by cooling of melted Tl_2TeO_5 samples.

When the $TiO_{0.5}$ content is higher than 50 mol%, α - $Tl_2Te_2O_5$ and Tl_2TeO_3 crystals are formed simultaneously from 150 °C. Their quantity increases until 320 °C, above which temperature they disappear by melting (Fig. 7).

Apart from the $Tl_2Te_2O_5$ samples, all melted samples remain vitreous after *in situ* fast-cooling at room temperature in the XRD device.

We are grateful to the Conseil Régional du Limousin for financial support.

References

- 1 A. K. Yakhkind, *J. Am. Ceram. Soc.*, 1966, **49**, 670.
- 2 H. Takebe, S. Fujino and K. Morinaga, *J. Am. Ceram. Soc.*, 1994, **77**, 2455.
- 3 R. Pressigout and B. Frit, *Rev. Chim. Minér.*, 1977, **14**, 300.
- 4 W. Vogel, H. Bürger, F. Folger, R. Oehrling, G. Winterstein, H. G. Ratzemberger and C. Ludwig, *Silicatechnik*, 1974, **25**, 206.
- 5 N. Mochida, K. Takahashi, K. Nakata and S. Shibusawa, *Yogyo-Kyokai-Shi*, 1978, **86**, 317.
- 6 T. Sekiya, N. Mochida, A. Ohtsuka and M. Tonokawa, *J. Non-Cryst. Solids*, 1992, **144**, 128.
- 7 J. Dexpert-Ghys, B. Piriou, S. Rossignol, J. M. Réau, B. Tanguy, J. J. Videau and J. Portier, *J. Non-Cryst. Solids*, 1994, **170**, 167.
- 8 T. M. Pavlova, K. K. Samplavskaya, M. Kh. Karapet'yants and Y. M. Khozhainov, *Russ. J. Inorg. Mater.*, 1976, **12**, 1891.

Paper 7/07554E; Received 20th October, 1997